Contribution to modeling of parasitic couplings for predicting EMC behavior of electrical machines

Jose Ioav Ramos Chavez, Jean-Marc Diénot, Paul-Etienne Vidal, Christophe Viguier, Bertrand Nogarède

Contribution to Modeling of Parasitic Couplings for Predicting EMC Behavior of Electrical Machines

J. I. Ramos, J-M. Dienot, P-E. Vidal, C.Viguier, B. Nogarède

***Abstract* – The characterization of parasitic couplings contributing to mechatronic assemblies' wide band Electromagnetic Compatibility (EMC) behavior is complex but increasingly essential for meeting needed performance and regulations. This article presents a comparative study of analytical and numerical approaches to determine the capacitive couplings in wound structures as an effort to develop a comprehensive approach to predict and prevent undesired couplings. The approach is based on physical and structural parameters analysis instead of behavioral characterization, allowing the use of predictive tools in the early design stage of mechatronic systems. The analytical model presented is compared to simulation methods applied to a three-layer inductor. Calculations converge to similar results. In the last part of the work, an experimental measurement of stray capacitance is done on an actual stator winding and compared to the analytical predictions of parasitic capacitances.**

I. INTRODUCTION

A. Association of Inverter, Cablings and Electrical Machine Effects Considerations

THE use of inverters with Pulse Width Modulation (PWM) control induces voltage waveform with fast rising/falling slopes. The developments on new semiconductor technologies such as SiC (Silicon Carbide) lead, among others, to increase the PWM switching times. The presence of parasitic elements (inductance, resistance and capacitance) in the inverter, cablings and actuators contribute Common Mode (CM) and Differential Mode (DM) currents, and therefore specific EMC behaviors. Furthermore, over-voltages appear at the electrical machine level which can be destructive for the winding (premature aging of insulation, partial discharge in dielectric materials…).

In Fig. 1 a typical waveform of the CM voltage of a PWM inverter and the CM currents at the different levels (inverter, cables and machine) are illustrated. Harmonics related to the PWM frequency (10 kHz) and the switching time (rising: 100 ns, falling: 500 ns, up to 1 MHz equivalent frequency) can be observed. In some configurations, long length cables between the inverter and the electrical machine, may cause the CM currents to be higher than the limit given by standards (as DO160 in aeronautical), and overvoltage (up to 2 times the rated voltage) to occur in machines' input as shown in Fig. 2.

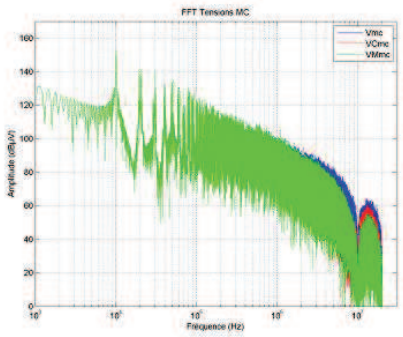

(a) CM Voltages

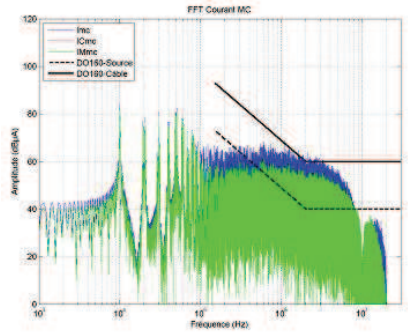

(b) CM Currents

Fig. 1 CM voltages/ currents with short cable (0.5 m) Vmc/Imc: inverter, VCmc/ICmc: cable, VMmc/IMmc: electrical machine. Novatem SAS ©.

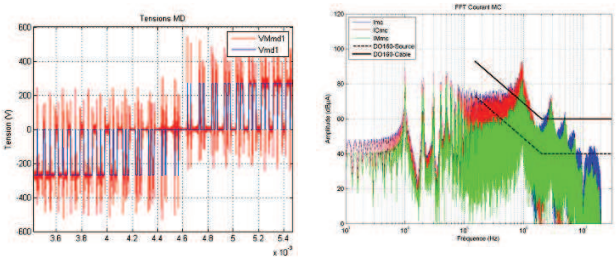

(a) DM Voltages (b) CM Currents

Fig. 2. DM voltages and CM currents with long length cable (50 m) Vmd1: inverter, VMmd1: electrical machine. Novatem SAS ©.

To anticipate and reduce the CM and DM voltages/currents, it is essential to know the wide band behavior of the different elements of the mechatronic architecture, to reduce either the causes or the consequences of potential Electromagnetic Interferences (EMI) issues. Modeling the parasitic couplings in both actuator and inverter, as well as cablings is helpful in anticipating potential couplings, even from the design phase.

This research work is supported by Novatem SAS, *Advanced Mechatronics*. 3 rue Merlin de Thionville, 11111-FR, Coursan.
Scientific resources have been supported by the EMI/EMC Plat-form LABCEEM, University P. Sabatier, FR-65000 Tarbes (jm.dienot@iut-tarbes.fr).

J. I. Ramos, Dr. Eng. C. Viguier and Pr. Dr. Eng. B. Nogarède work with Novatem SAS, Advanced Mechatronics, Toulouse, FRANCE, 3 rue Merlin de Thionville, 11111-FR, Coursan. (ji.ramosch@novatem-sas.com)
Pr. Dr. J-M. Dienot and Dr. Eng. P-E. Vidal are with the Laboratoire Génie de Production in the Electrical Engineering Department at INP-ENIT, Toulouse University, 47 av. d'Azeirex, 65000-FR, Tarbes.

B. *Wide Band Frequency Impedance of Electrical Machines*

Experimental impedance measures in DM and CM are often carried out to characterize the overall machine behavior. These results are currently used to fit behavioral models as shown in Fig. 3 and Fig. 4 (b).

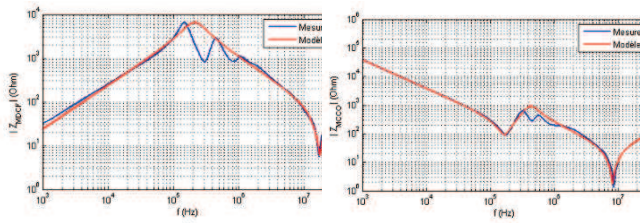

(a) Differential Mode (b) Common Mode

Fig. 3. EM typical behavior (CM, DM) – Novatem SAS ©

Moreover, High Frequency (HF) models of the electrical machine have been developed. To sum them up, two types of model are often proposed (Fig. 4):

- Temporal approach: use of the transmission line theory (TLM) [1],[2]. For windings with high number of turns, the equivalent matrix inserted in the differential equation to solve the voltage/current relation is consequently large. Consequently, the time resolution of the problem taking into account the switching times is important. Furthermore, this method does not take into account the magnetic coupling between the different phases.
- Frequency approach: use of an equivalent electrical circuit (EEC) of the electrical machine [3]–[6]. Parameters of the electrical circuit are determined from experimental measures by identification.

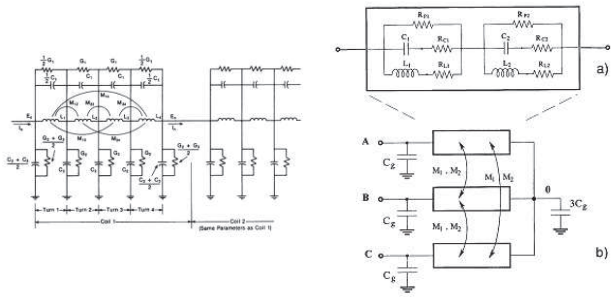

(a) TLM Approach [1] (b) EEC Approach [5]

Fig. 4. Example of EM modeling in HF (CM, DM)

C. *Physical and Structural Parameters for Preliminary EMC Prediction and Design Purposes*

The aim of this work is to contribute to the development of a modeling methodology of the electrical machine in the High Frequency domain taking into account the physical and geometrical parameters of windings. This approach will allow integration of EMC performance from the first step of a mechatronic design to prevent and predict susceptibility and emission levels from a comprehensive view of the global system.

This paper is specifically focused on modeling parasitic capacitive couplings in symmetrical and regular wound inductors, as an essential phase to understand the structural parameters contributing to wide band EMC behavior. Different approaches are presented and discussed.

II. CONTRIBUTION TO PARAMETERIZATION OF PARASITIC CAPACITANCE IN ELECTRICAL MOTORS

The analytical model of parasitic capacitance between turns and core of wound structures is compared to simulation results of capacitance calculations. The analytical model can then be integrated into a design and optimization loop for predicting EMC and HF behavior of electrical actuators, from 0Hz up to 100MHz.

A. *Analytical Modeling of Parasitic Capacitance in Wound Structures*

The analytical work presented is based on the work carried out by A. Massarini [7], [8].

1) General modeling and considerations

A multilayer iron-cored solenoid architecture is considered. Fig. 5 shows a cross-sectional view of several copper wire turns with their respective coating thickness. Turn-to-turn and turn-to-core capacitance calculations are described.

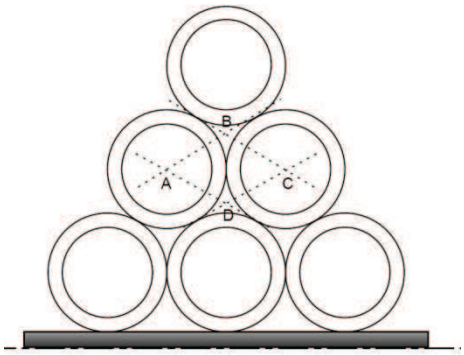

Fig. 5. Cross-sectional partial view of a multilayer inductor

Three couplings can be identified:

- Turn-to-turn capacitance of turns in the same layer
- Turn-to-turn capacitance of turns in different layers
- Turn-to-core capacitance

Because of symmetries, electric field lines are considered to be equally shared between adjacent conductors of the inner layers[7].

For the inner layers, the calculation of turn-to-turn capacitance can be reduced to the analysis of the ABCD cell representing the assumed electric field lines mean paths between two turns because of symmetries[8].

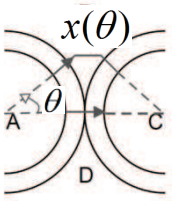

Fig. 6. Assumed path x for field lines between adjacent conductors for $-\pi/6 \leq \theta \leq \pi/6$.

Since surfaces are considered to be perfect equipotentials, electric field lines are orthogonal to the conductor surfaces.

The paths are then depicted for the field lines: lines from one turn to another go through a coating thickness, then trough air and through coating thickness again. Since the thickness *e* is small to wire diameter *Dc*, lines in the coatings are considered to be orthogonal to the conductor surface as shown in Fig. 6. Because of the proximity effect, electric field lines are concentrated around the shortest distance between two different equipotentials. Thus, E lines are considered to be parallel and close to small values of θ as shown in Fig. 6. It is then assumed that for adjacent turns, the flux lines are exclusively directed towards the next immediate conductor. Capacitance for non-adjacent turns is not taken into account.

As a first approximation, for the most external layer, because of the proximity effect, electric field lines between turns of the layer are assumed to be shared in the same way that for the turns of the inner layers. For the first layer adjacent to the core, the lines between turns are also considered to be shared equally than for the inner layers[8].

The turn-to-turn capacitance is then considered to be the same for all adjacent turns of any layer.

2) Turn-to-turn Capacitance for Inner Layers

In Fig. 7 and Table I are shown the parametric dimensions of the solenoid structure:

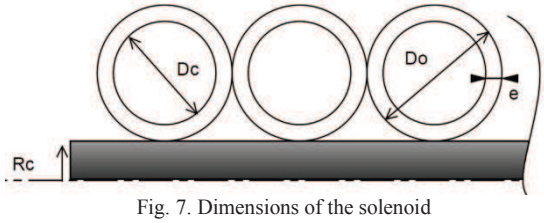

Fig. 7. Dimensions of the solenoid

TABLE I
SOLENOID GEOMETRICAL PARAMETERS

Rc	Iron core radius
Dc	Copper wire diameter
Do	Outer diameter of wire
e	Coating thickness

The elementary capacitance *dC* between the equivalent elementary surfaces *dS* of two adjacent conductors can be described as:

$$dC = \varepsilon \frac{dS}{x} \tag{1}$$

The capacitance along the coupling paths (coating of the first turn) can then be calculated:

$$dCc = \varepsilon \frac{lt}{\ln\left(\frac{r_0}{r_c}\right)} d\theta \tag{2}$$

In numerical calculations, the length of a turn *lt* is here approximated to its perimeter. For the air gap, the capacitance can be calculated considering that in this region, $x(\theta)=Do(1-\cos\theta)$.

$$dCg = \varepsilon_0 \frac{lt}{2(1 \quad \cos\theta)} d\theta \tag{3}$$

Finally, for the third segment concerning E lines entering the coating of the second conductor, the capacitance is the same as in (2), as for the first coating.
Thus, the total turn-to-turn capacitance can be written as

$$Ctt = Cg + 2Cc \tag{4}$$

3) Turn-to-core capacitance and total stray Capacitance Cs of the winding

For the inner layer, the turn-to core capacitance can easily be calculated with the same expressions. Considering the iron core surface as a perfect equipotential, electric field lines are orthogonal to the surface of the core. In that case, turn-to-core electric field lines go through half of the path compared to the turn-to-turn lines [7]. As a first approximation, the surface taken by the electric field lines is considered to be the same as for the turn-to-turn capacitance. In that case, the resulting capacitance is then

$$Ctc = 2Ctt \tag{5}$$

Moreover, the analytical model developed by A. Massarini in [7] and [8] helps predicting the *Cs* value for structures for up to 3 layers. In that work, it is assumed that we can calculate *Cs* by multiplying *Ctt* by a *k* factor which can be found with intricate series convergence. However, only the case of a one-layer iron-cored solenoid was experimentally verified.

B. Capacitance Matrix Extraction Using the PEEC Method and Finite Element Analysis (FEA)

1) The PEEC Method and Parameters Extraction

PEEC method, for Partial Element Equivalent Circuit, is based on an integral electromagnetic formulation describing the geometry and interpreted in terms of L, C, and R circuit elements. It provides a correlation of the field calculation and the circuit interpretation [10]. Summation of all sources of electric field within a conductor leads to the expression of the external field applied:

$$\vec{E}_0 = \frac{\vec{J}(\vec{r},t)}{\sigma} + \frac{\partial \vec{A}(\vec{r},t)}{\partial t} + \nabla\Phi(\vec{r},t) \tag{6}$$

Where $\vec{r}$ is the vector from the origin and $\vec{E}_0$ an external field for a system of K conductors and regions of uniform ε_r, μ_r; c being the speed of light. In absence of external field applied, (6) can be expressed as:

$$0 = \frac{1}{\sigma}\int_{v_l} \vec{J}_\gamma(\vec{r},t)dv_l + \sum_{k=1}^{K}\sum_{n=1}^{N_{nk}} \frac{\mu}{4\pi}\left[\int_{v_l}\int_{vnk} G(\vec{r},\vec{r}')dv'dv_l\right]\frac{\partial \vec{J}_{\gamma nk}(t_n)}{\partial t} + \sum_{k=1}^{K}\frac{1}{4\pi\varepsilon}\int_{v_l}\frac{\partial}{\partial\gamma}\left[\int_{vk} G(\vec{r},\vec{r}')q(\vec{r}',t')ds'\right]dv_l \quad (7)$$

t' is considered to be the retardation time between the source point $\vec{r}'$ and the observation point $\vec{r}$. The unknown quantities then are the current density J in conductors and density of charges q on the surfaces. In order to solve the system of equations derived from (7), current densities are discretized into N volume cells, giving the overall current flow for each one of K conductors, then by defining local cell current densities as a pulse function in the three dimensional directions $\gamma = x, y, z$ [9], [10]. As for the density of charges, they are defined on the conductor surfaces and expressed as pulse functions as well for M surface cells. In the case of perfect conductors for capacitance calculation, absence of external electric field and aforementioned unknown quantities being locally constant (more general cases are detailed in[11], [12]). Then, (7) is interpreted in terms of voltage drops and thus, circuit impedance elements[9].

Capacitance (C), Inductance (L) and Resistance (R) matrixes are then determined for a system of K conductors. These matrixes represent the main and parasitic coupling parameters. They can be exported in a Spice Netlist format for further circuit analysis. The Netlist is then imported as a subcircuit whose ports are functional conductors or nets defined in the 3D model and connected to a complete circuit for larger circuit analysis. Fig. 8 shows the general form of the extracted capacitive elements in terms of partial self and mutual capacitance for K conductors:

$$C_T = \begin{bmatrix} C_1 & \dots & C_{1j} & C_{1K} \\ \vdots & \ddots & & \vdots \\ C_{i1} & & C_i & \\ C_{K1} & \dots & & C_K \end{bmatrix}$$

Fig. 8. Extracted capacitance matrix with partial self and mutual values

The software used for the parameters extraction is Q3D®. Q3D® is a fixed frequency complete multi-material field analysis software based on the PEEC method taking into account mechanical and electrical layout of a structure[13].

C. Finite Element Analysis of Turn-to-turn and Turn-to-core Capacitance

The 2D model of the inductor is used to calculate the electrostatic field between conductors. The stored electrostatic energy *We* in the divided zones between conductors is computed once the electrostatic field is calculated. The capacitance can be obtained, since

$$Cm = 2We / V^2 \text{ in F/m} \quad (8)$$

V being the voltage difference applied to the concerned copper conductors for capacitance calculation.

III. Case Study of a Three-Layer Iron-Cored Inductor

The inductor modeled is a three-layer solenoid with an iron core and five jointed turns per layer as shown in Fig. 9.

A. Inductor Structure Description and Materials

TABLE II
Solenoid Geometrical Description

Rc	Iron core radius	10 mm
Dc	Copper wire diameter	1.5 mm
Do	Outer diameter of wire	1.6 mm
e	Coating thickness	0.05 mm
lt	Turn length	Calculated for each layer

TABLE III
Material Properties

Conductivity of copper	σ_c=58 000 000 S/m
Relative permeability of copper	μ_c=0.99991
Relative permittivity of coating material	ε_r=3.5
Relative permeability of iron core	μ_i=4000
Conductivity of iron core	σ_i=10 300 000 S/m

B. Comparison of Analytical Calculations and Simulation

1) Analytical results

The analytical calculations of turn-to-turn capacitance (*Ctt*) according to the hypotheses established in the precedent paragraph are resumed in Table IV:

TABLE IV
Analytical Computation of Turn-to-Turn Capacitance (*Ctt*)

Layer	***Ctt*** (average values for the 5 turns per layer in pF)
1 *(lt=67.86mm)*	7.65
2 *(lt=76.56mm)*	8.63
3 *(lt=85.27mm)*	9.61
1-2 *(lt~72.88mm)*	8.21
2-3 *(lt~81.6mm)*	9.16

The turn-to-core capacitance is only calculated for the first layer since the E lines are considered to be shared only between immediate adjacent conductors. Thus, turn-to-core capacitance is ***Ctc*=15.30 pF**.

2) Parasitic Capacitance Parameters Extraction and 2D Finite Element Analysis Results

The solenoid was modeled in a 3D modeler and imported into Q3D Extractor® for partial self and mutual capacitance extraction. Turns of the inductor are isolated from one another in order to consider them separate conductors. As shown in Fig. 9, turns have thus been drawn as toroidal independent turns instead of a helical structure. Only the capacitance calculation has been carried out. The partial self and mutual capacitances between turns and turns and core have been exported as a matrix [7].

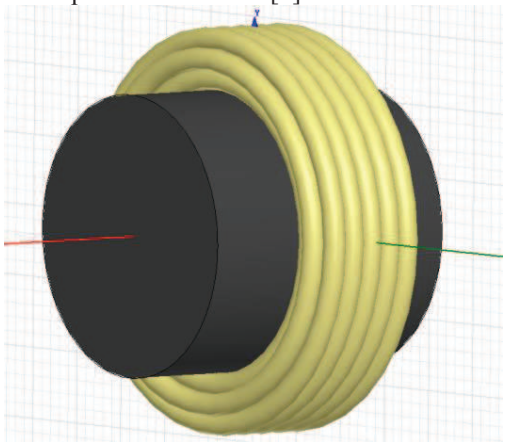

Fig. 9. 3D model of the three-layer iron-cored inductor for PEEC simulation

For the Finite Element calculations, the 2D geometry has been divided into equally separated zones around turns considering the hypothesis that electric field lines are shared equally between adjacent conductors as showed in Fig 10. The result is then multiplied by the turn length as a first approximation.

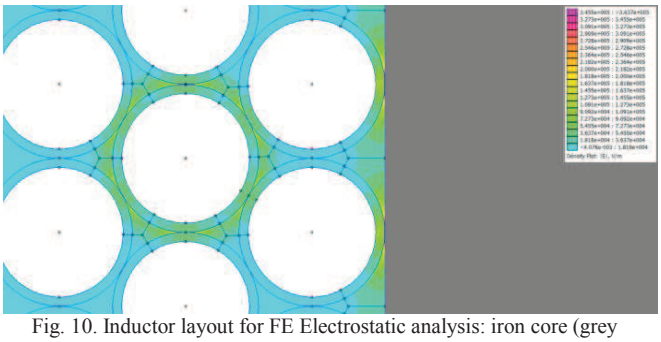

Fig. 10. Inductor layout for FE Electrostatic analysis: iron core (grey zone), copper turns (white circles) surrounded by a coating thickness. Coatings and surrounding air divided for energy computation.

C. Results Comparison and Analysis

Average values of turn-to-turn (*Ctt*) and turn-to-core (*Ctc*) capacitances for immediate adjacent conductors are resumed in Table V.

TABLE V
TURN-TO-TURN AND TURN-TO-CORE CAPACITANCE COMPUTED VALUES FOR ADJACENT TURNS AND CORE

Capacitance (pF)	Analytical	Partial Capacitance Extraction in 3D (PEEC)	Energy Calculation in 2D (FEA)
Ctt *Layers 1to1*	7.65	4.25	5.23
Ctt *Layers 2 to 2*	8.63	8.11	5.90
Ctt *Layers 3 to 3*	9.61	9.53	6.57
Ctt *Layers 1 to 2*	8.21	7.41	5.61
Ctt *Layers 2 to 3*	9.16	7.68	6.26
Ctc *Layer 1 to core*	15.30	52.55	11.97

For non-adjacent turns and core, average results are resumed in Table VI.

TABLE VI
TURN-TO-TURN AND TURN-TO-CORE CAPACITANCE COMPUTED VALUES FOR ADJACENT TURNS AND CORE

Capacitance (pF)	Analytical	Partial Capacitance Extraction in 3D (PEEC)	Energy Calculation in 2D (FEA)
Ctt *for immediate non- adjacent turns of the same layer*	0	0.007	0.035
Ctt *for immediate non-adjacent turns of the external layer*	0	0.078	0.031
Ctt *for immediate non-adjacent turns between layer 1 and 3*	0	0.01	0.038

The overall tendencies of computed turn-to-turn capacitances are similar. The three methods converge to similar conclusions concerning the hypothesis stated for the analytical model established in[7], [8]. Electric flux lines are mostly shared between immediate adjacent turns. Table VI shows that non-adjacent turns capacitances can be neglected, since capacitances represent at most 10% in the worst case scenario when compared to adjacent turn-to-turn. For the external layer, proximity effect actually concentrates lines in the same way that for inner layers. Table VII shows the relative error between simulation and analytical solutions.

TABLE VII
RELATIVE ERROR COMPARISON FOR CTT AND CTC COMPUTED VALUES

Relative Error	Parameters Extraction to Analytical	FEA to Analytical
Ctt *same layer (average)*	19 %	32 %
Ctt *different layers (average)*	14 %	32 %
Ctc *layer 1 to core (average)*	240 %	22 %

The global accuracy of the analytical model compared to simulation techniques is questionable regarding the relative

error. However, considering the elevated number of hypotheses assumed in precedent paragraphs, results are encouraging and converge to the same orders of magnitude. The *Ctc* value for PEEC (parameters extraction) method is nevertheless far from the other two methods. Q3D® and its meshing algorithm are not optimized for toroidal and helical structures with thin coats of materials. They were originally built to test PCB structures and IC packaging. Results for turn-to-turn capacitances were stable and highly accurate for several tests but this was not the case for turn-to-core capacitances.

The FE analysis allowed observing the turn-to-core coupling mechanism with great detail. The hypothesis stated in [8] in which electric flux lines go through half the path that the path for turn-to-turn is verified, but the surface of the turn-to-core taken by E lines is larger than the turn-to-turn one. Thus, *Ctc* can be approximated to 2.4 to 3 times *Ctt* according to FE analysis.

IV. Experimentation Setup for Model Validation

A. Experimental test bench

The test bench designed for measuring parasitic couplings in wound structures is composed by otherwise high frequency equipment and frequency behavior of all cablings, connections and measuring components is accurately determined. Fig. 11 shows the layout of the test bench. The modularity of the bench is aimed as a complement for a typical 4294A-like Impedance Analyzer. The wide variety of *devices under test* (DUT) and their different connection leads require specific fixturing. To take into account the high-frequency behavior of the DUT's environment, specific Printed Circuit Boards (PCB) for the dipole characterization were designed and optimized in terms of impedance. The method of characterization of the PCBs is based on the Virtual Experimentation (XVICE) Method, described in [14] and [15], in which partial self and mutual elements (R,L and C) are extracted with the PEEC method and exported into a SPICE environment for circuit analysis and simulation. XVICE allow optimal electromagnetic behavior prediction for complex electrical structures, since, once the environment completely known, several DUTs can be tested and simulated for analysis with outstanding efficiency [14].

Special attention was appointed to the bandwidth of measuring equipment as well as for the coaxial cables used to connect the devices. Considering the 100MHz upper limit of characterization procedures, current (CT-1 Tektronix) and voltage (Lecroy AP020) probes have a limit operation frequency of 1GHz. These probes have also very low insertion losses on a wide band of frequency, by the way of very low equivalent parasitic elements. Coaxial cables and connectors (rated 1GHz) are used to minimize the impact of cablings, and are as electrically short at the range of frequency used for the experiment: the retardation effects are considered to appear starting from about 20cm at 100MHz. To complete this, a high-speed wide-band Digital Oscilloscope (Lecroy LC564A, 1GHz) is used to visualize and acquire signals from current and voltages probes.
The experiment, completed with a performing harmonic source (1GHz, T_{HD} < 0,05%, 1mW-10W) is driven by a GPIB programmed interfaces and network. Accurate acquisition, post-treatment and export of the conditions and results of the characterization allow pertinent and fine validation of the experiment.

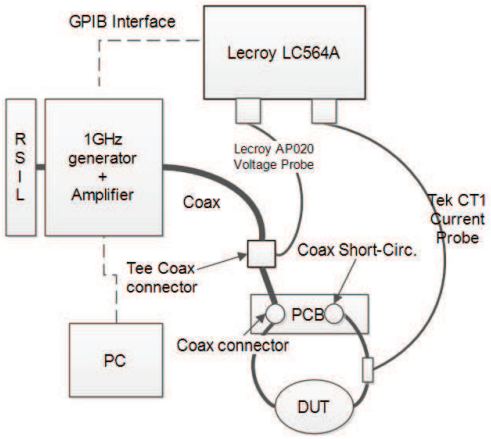

Fig. 11. Wide Band Test Bench for EMC Characterization

B. First results with an actual motor winding structure

The winding under test is a 7-layer and 14 turns per layer winding stator module used for a 20 kW fault-tolerant modular electric motor for vehicle traction patented by NOVATEM. Fig. 12 shows the wires wound in a regular way around the pole. The center of the pole supporting the winding has a rectangular cross section with rounded corners, which differs from the shape used in previous parts of the paper. Besides, the pole has a particular shape causing the external turns of each layer to be adjacent to the core. However, with similar hypotheses as for the analytical calculations, we can show that the only changing factor is the turn length and for the external turns of each layer in contact of the core over a certain length, we consider the same behavior of turn-to-core capacitance as for the inner turns against the central core. Symmetries and invariances are conserved so hypotheses are the same. The wire used was regularly wound around the stator module. The copper wire has a diameter of 1 mm and a 0.12 mm coating thickness. The turn length is calculated for each layer knowing that for the inner layer the length is 140.2 mm. The coating has a relative permittivity of 3.5.

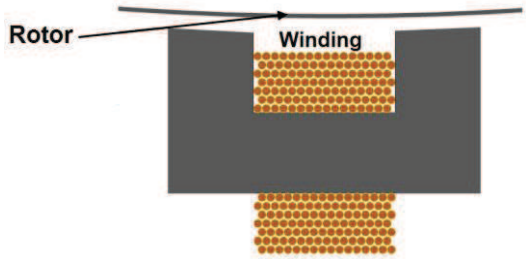

Fig. 12 Partial cross sectional illustration of the stator with the concentric winding.

From impedance measurements from 10 kHz up to 100MHz, the extracted stray capacitance was calculated at resonance, knowing the inductance value of the winding module. Finally, the measured total stray capacitance *Cs* is **18.3 pF**. Then, the analytical values of *Ctt* (**10.9 pF** for the first layer) and *Ctc* (**21.8 pF** for the inner layer) were calculated. In order to correlate these values to the measured total stray capacitance, instead of calculating the convergence of the numerical series as in [7] and [8], an equivalent circuit SPICE model of the capacitance network has been created

using the analytical *Ctt* and *Ctc* values for each layer. The resulting estimated value of stray capacitance, with the analytical values inserted in SPICE simulation, is **17.9 pF** which is barely **2%** lower than the measured one.

V. CONCLUSIONS

An effort to understand and find predictive methods of the turn-to-turn and turn-to-core capacitance mechanism with real structural, geometrical and material parameters is presented. The first is an analytical method. The second, is based on the PEEC parameters extraction and the last is a Finite Element analysis method. Instead of a benchmarking demarche, the three methods are presented as complementary tools for analysis. Specifically, an effort to validate some hypothesis stated in the analytical model is done. In this first phase of the work, simple winding geometries are considered. An experimental measurement is confronted to an estimation of the total stray capacitance of an actual motor winding by the means of the analytical model and a circuit simulator tool. Only the analytical values and hypotheses are used for the circuit simulation. The results are staggeringly close to each other for the winding under test. The analytical model seems to predict very accurately the turn-to-turn and core mechanism, but further validation is required. In fact, FE analysis predicted a slight increase in *Ctc* estimations, and that impact must be evaluated experimentally. Then, the capacitance network (the same predicted by the analytical method in [7] and [8]) implanted into a SPICE simulator is complex but it avoids using complex tools for convergence calculations. This method is not very efficient if larger numbers of turns per windings are considered, so more performant tools must be considered for larger windings.

VI. REFERENCES

[1] R. G. Rhudy, E. L. Owen, and D. K. Sharma, "Voltage Distribution Among the Coils and Turns of a Form Wound AC Rotating Machine Exposed to Impulse Voltage," *IEEE Power Eng. Rev.*, vol. PER-6, no. 6, pp. 40–41, Jun. 1986.

[2] G. Grandi, D. Casadei, and U. Reggiani, "Equivalent circuit of mush wound AC windings for high frequency analysis," in *, Proceedings of the IEEE International Symposium on Industrial Electronics, 1997. ISIE '97*, 1997, vol. 1, pp. SS201–SS206 vol.1.

[3] G. Skibinski, R. Kerkman, D. Leggate, J. Pankau, and D. Schlegel, "Reflected wave modeling techniques for PWM AC motor drives," in *Applied Power Electronics Conference and Exposition, 1998. APEC '98. Conference Proceedings 1998., Thirteenth Annual*, 1998, vol. 2, pp. 1021–1029 vol.2.

[4] F. Costa, C. Vollaire, and R. Meuret, "Modeling of conducted common mode perturbations in variable-speed drive systems," *IEEE Trans. Electromagn. Compat.*, vol. 47, no. 4, pp. 1012–1021, Nov. 2005.

[5] G. Grandi, D. Casadei, and U. Reggiani, "Common- and differential-mode HF current components in AC motors supplied by voltage source inverters," *IEEE Trans. Power Electron.*, vol. 19, no. 1, pp. 16–24, Jan. 2004.

[6] A. F. Moreira, T. A. Lipo, G. Venkataramanan, and S. Bernet, "High-frequency modeling for cable and induction motor overvoltage studies in long cable drives," *IEEE Trans. Ind. Appl.*, vol. 38, no. 5, pp. 1297–1306, Sep. 2002.

[7] A. Massarini, M. K. Kazimierczuk, and G. Grandi, "Lumped parameter models for single- and multiple-layer inductors," in *, 27th Annual IEEE Power Electronics Specialists Conference, 1996. PESC '96 Record*, 1996, vol. 1, pp. 295–301 vol.1.

[8] A. Massarini and M. K. Kazimierczuk, "Self-capacitance of inductors," *IEEE Trans. Power Electron.*, vol. 12, no. 4, pp. 671–676, Jul. 1997.

[9] A. E. Ruehli, "Equivalent Circuit Models for Three-Dimensional Multiconductor Systems," *IEEE Trans. Microw. Theory Tech.*, vol. 22, no. 3, pp. 216–221, Mar. 1974.

[10] A. F. Peterson, S. L. Ray, and R. Mittra, *Computational Methods for Electromagnetics*. Wiley, 1998.

[11] A. E. Ruehli and H. Heeb, "Circuit models for three-dimensional geometries including dielectrics," *IEEE Trans. Microw. Theory Tech.*, vol. 40, no. 7, pp. 1507–1516, Jul. 1992.

[12] G.-L. Li and Z.-H. Feng, "Consider the losses of dielectric in PEEC," in *2002 3rd International Conference on Microwave and Millimeter Wave Technology, 2002. Proceedings. ICMMT 2002*, 2002, pp. 793–796.

[13] "Q3D Technical Notes, Maxwell 3D Technical Notes." ANSOFT, 2001.

[14] E. Batista and J.-M. Dienot, "EMC characterization for switching noise investigation on power transistors," in *IEEE International Symposium on Electromagnetic Compatibility, 2008. EMC 2008*, 2008, pp. 1–7.

[15] J. I. Ramos, J.-M. Dienot, P.-E. Vidal, B. Nogarède, C. Viguier, and E. Batista, "Virtual Experimentation for EMC Parameters Extraction: Case of the Parasitic Capacitance in Wound Structures," *11th Int. Conf. Model. Simul. Electr. Mach. Convert. Syst.*, May 2014.

VII. BIOGRAPHIES

José Ioav RAMOS CHAVEZ was born in Mexico City in 1988 and obtained his Electrical Engineering and Automation diploma in 2012 from the ENSEEIHT Engineering School of the Institut National Polytechnique of Toulouse (INPT), France. He currently is a second year Ph.D. student at INPT sponsored by NOVATEM SAS (www.novatem-sas.com) and in collaboration with Laboratoire Génie de Production (LGP) and LABCEEM platform in Tarbes, France. His work concerns the study of EMC and wide-band behavior of mechatronic systems and electrical systems in general.

Jean-Marc DIENOT received PhD degrees in Microwave Circuits and Applied Electromagnetic, from the University Paul Sabatier, Toulouse, France. He is currently a University Professor in the Institute of Technology, Tarbes, France. Since 1995, he has been interested and involved by new Electromagnetic Interferences problematic in Electronics' architectures. He has developed and leads the LABCEEM platform, dedicated for research and high-level trainings projects in EMI and EMC domains. He is author or co-author of about ninety contributions in Journals, Books and Conferences. He is recipient of scientific certifications and committee's member in domains as Power Electronics, EMC, Instrumentation and Communications.

Paul-Etienne VIDAL obtained a Ph.D. degree from INPT in 2004. From 2004 to 2006, he was engaged as Temporary Researcher at the laboratory LEEI, INP/Centre National de la Recherche Scientifique (CNRS), where he worked on electrical machine controls and multi-machine multi-converters systems. Since 2006 he is an associate professor at LGP –University of Toulouse. His research topic deals with power converter efficiency. He developed 3 research themes: electro thermo mechanical modeling and simulations; experimental test devices; and improved power converter drives. A significant amount of his research is done within the PRIMES platform (www.primes-innovation.com/) facilities.

Christophe VIGUIER was born in Castres, France, in 1978. He received the M.S. degree in Automation, Electronics and Electrical Engineering from the University Paul Sabatier of Toulouse, France, in 2001. He received PhD degree in electrical engineering from the INPT in 2005. He is currently R&D Engineer at NOVATEM SAS which carries development projects of embedded innovative equipment in electrical engineering. His current work includes study, modelling and design of electromechanical actuators, from electroactive materials to electromagnetic devices.

Bertrand NOGAREDE was born in Montpellier, France, in 1964. He received the Engineering degree in electrical engineering from the ENSEEIHT, Toulouse, France, in 1987 and the Ph.D. degree from the INPT in 1990. He is a University Professor at INPT. He is currently the Scientific and Technical coordinator at NOVATEM SAS. Author of *Electrodynamique Appliquée (Dunod, 2005)*, he has worked on modeling and design of electrical innovative machines using, analytical field calculation methods and optimization techniques including fault-tolerant and high speed machines, among others, for performance applications in aeronautical, medical and automotive industry. Among his various awards, he is laureate of the 2007 Blondel Medal.